Evolution of beta-lactam resistance causes fitness reductions and several cases of collateral sensitivities in the human pathogen *Haemophilus influenzae*

Sabine Petersen[1], Margo Diricks[2,3], Christian Utpatel [2], Hinrich Schulenburg[4,5], Matthias Merker[1,3]

[1] Evolution of the Resistome, Research Center Borstel, Borstel, Germany

[2] Molecular and experimental Mycobacteriology, Research Center Borstel, Borstel, Germany

[3] German Center for Infection Research, Partner site Hamburg-Lübeck-Borstel-Riems, Borstel-Lübeck, Germany

[4] Evolutionary Ecology and Genetics, Kiel University, Kiel, Germany

[5] Antibiotic Resistance Group, Max-Planck Institute for Evolutionary Biology, Ploen, Germany

Correspondence to: Prof. Matthias Merker, Research Center Borstel, Leibniz Lung Center, Parkallee 1, 23845 Borstel, phone: +49-4537188-7570, e-mail: mmerker@fz-borstel.de

Short title: β-lactam Resistance Drives Trade-offs in H. influenzae

Transparency declarations: The authors declare that they do not have any competing interests.

Keywords: Haemophilus influenzae, ampicillin resistance, cephalosporine resistance, evolution of antimicrobial resistance, collateral effects

Abstract

The evolution of antimicrobial resistant (AMR) pathogens poses a global health threat and it is unclear if evolutionary trajectories to resistance lead to predictable phenotypes. We analyzed AMR-evolution in the human pathogen *Haemophilus influenzae* in controlled evolution experiments with increasing concentrations of either ampicillin, cefotaxime, or ceftriaxone. We isolated 315 clones from different time points of six independent experiments and characterized changes in genome sequences, bacterial fitness, and minimum inhibitory concentrations (MICs) to 14 antibiotics. Resistance evolution under ampicillin and cefotaxime was mainly driven by mutations in the *ftsI* gene, encoding the penicillin-binding protein 3. However, ceftriaxone exposure repeatedly selected for amino acid substitutions in the outer membrane protein P2 (OmpP2). Some OmpP2-mutants reproducibly showed phenotypic heterogeneity for ceftriaxone but also for fluoroquinolones, rifampicin and tetracycline. Bacterial fitness assessments revealed trade-offs between resistance-associated mutations and growth, though no systematic correlation of MIC increase and growth deficit was detected. Over 50% of the selected clones became more susceptible to aminoglycosides, clarithromycin, and colistin, while some mutation patterns resulted in cross-resistance to meropenem and fluoroquinolones. Overall, beta-lactam antibiotics reproducibly selected mutants with increased MICs, but evolutionary pathways and resulting phenotypes remain unpredictable. These findings highlight the complexity of resistance evolution and suggest that future AMR treatment strategies may need to consider strain-specific and collateral effects more closely.

Introduction

Antimicrobial resistance (AMR) is a major public health challenge globally (1). The WHO has identified several priority pathogens to inform research and development as well as public health interventions to combat the AMR crisis (2). One of these priority pathogens are ampicillin resistant *Haemophilus influenzae* strains. *H. influenzae* is a common Gram-negative opportunistic pathogen residing in the human upper respiratory tract (3,4). The bacterium can cause a range of infections, from mild illnesses like sinusitis and otitis media to severe invasive diseases such as meningitis and bacteremia, particularly in vulnerable populations (5). Despite the successful implementation of a vaccine against *H. influenzae* serotype b strains, non-typeable strains (NTHi), i.e., strains lacking a polysaccharide capsule, have become prevalent (6) and evolved resistance to aminopenicillins such as ampicillin and amoxicillin in many world regions (7–9).

While amoxicillin-clavulanate and ampicillin-sulbactam are used worldwide to overcome beta-lactamase-mediated resistance (predominantly TEM-1 and ROB-1), third-generation cephalosporins such as cefotaxime and ceftriaxone also effectively bypass these enzymes (10,11) and are increasingly favored in clinical practice (12). This is due to their favorable tolerability and their ability to achieve high serum and cerebrospinal fluid concentrations, making them especially suitable for the treatment of severe infections like sepsis and meningitis caused by *H. influenzae* (13). However, resistance to beta-lactams can also evolve in beta-lactamase negative strains via alterations in the penicillin binding protein 3 (PBP3), encoded by the *ftsI* gene (14). Mutations in *ftsI*, particularly in the transpeptidase domain of PBP3, reduce the binding affinity for different beta-lactam antibiotics (15).

Current understanding is limited regarding whether resistance evolution in *H. influenzae* follows identical genetic and phenotypic trajectories across different beta-lactam classes, and whether such evolutionary pathways are reproducible. In particular, it is unclear if evolution consistently leads to cross-resistances against multiple beta-lactam antibiotics, or if variability in resistance mechanisms leads to diverse outcomes. Here, laboratory-based evolution experiments provide a powerful approach to address these questions (16). By simulating selective pressures *in vitro*, these experiments allow for tracking genetic changes and phenotypic adaptations as resistance evolves. In addition, this experimental approach facilitates an assessment of evolved collateral effects, such as cross-resistance or collateral sensitivity (i.e., variants with evolved resistance against certain antibiotics show an increase in susceptibility to other antibiotics), which may inform about epistatic interactions, and possibly new treatment regimens against resistant strains (17).

Therefore, the aim of the current study was to enhance our understanding of the predictability of resistance evolution and the resulting collateral effects. In particular, we investigated the evolutionary pathways leading to resistance against either ampicillin, cefotaxime, or ceftriaxone in *H. influenzae* using a multi-step *in vitro* evolution approach. By subjecting the reference strain *H.*

influenzae Rd KW20 to increasing concentrations of these antibiotics, we tested whether evolution results in identical or divergent genetic trajectories and phenotypes. We employ short- and long-read sequencing technologies to map mutations across the genome and assess their impact on minimum inhibitory concentrations (MICs) for different antibiotics. Furthermore, we evaluated whether the evolution of resistance is reproducible by examining the consistency of mutation patterns and collateral effects on other antibiotics.

Methods

Bacteria and culture methods

The beta-lactamase negative reference strain *H. influenzae* Rd KW20 and evolved mutant strains were routinely grown from −80°C freezer stocks on chocolate agar (Mueller-Hinton broth with 5 g/L yeast extract, 17 g/L agar, 5% defibrinated horse blood and 20 mg/L beta-nicotinamide adenine dinucleotide (beta-NAD)) at 37°C in a humid atmosphere containing 5% CO_2. Colonies grown on chocolate agar served as inoculum for liquid cultures in Mueller-Hinton broth supplemented with 5 g/L yeast extract, 20 mg/L beta-NAD and 15 mg/L hemin, hereafter referred to as *Haemophilus* test medium (HTM), grown at 37°C and shaking at 100 or 200 rpm. Liquid cultures were routinely plated on HTM agar (formulation of HTM with 17 g/L agar added).

Antibiotic susceptibility testing

To determine the antibiotic starting concentrations for the multi-step evolution experiment, MICs of ampicillin, cefotaxime and ceftriaxone were tested for the reference strain using broth microdilution methodology according to EUCAST protocol, but using HTM. Ampicillin sodium salt, cefotaxime sodium salt, and ceftriaxone disodium salt hemi(heptahydrate) were purchased from Sigma-Aldrich.

Gradient diffusion strips (Liofilchem® MIC Test Strips) on Mueller Hinton fastidious agar (MH-F, BD) were routinely used for all isolated single clones evolved in the evolution experiment to determine MICs of ampicillin, cefotaxime and ceftriaxone. To check for collateral effects, 17 clones (3–4 per evolved population, selected based on differing mutational patterns and/or distinct beta-lactam MICs) were additionally tested for clarithromycin, kanamycin, colistin, vancomycin, levofloxacin, rifampicin, amikacin, tetracycline, gentamicin and meropenem susceptibility using Liofilchem® MIC Test Strips. Susceptibility interpretation was performed according to EUCAST breakpoints v. 13.0 2023, which are 1 mg/L for ampicillin, 0.125 mg/L for cefotaxime, and 0.125 mg/L for ceftriaxone.

Multi-step evolution experiment

Populations of the susceptible reference strain *H. influenzae* Rd KW20 were evolved under antibiotic pressure (ampicillin, cefotaxime, ceftriaxone) in HTM, starting with an antibiotic concentration of 0.5xMIC of the reference strain (determined using broth microdilution methodology). One

124 population was evolved in the absence of any antibiotic pressure (control). Evolution in the presence
125 of ceftriaxone was performed three times to investigate reproducibility of resistance evolution.

126 A volume of 20 µL of single colony resuspension (one single colony of *H. influenzae* Rd KW20 grown
127 on chocolate agar resuspended in 100 µL of HTM) was used to inoculate 2-mL cultures containing
128 either 0.125 mg/L of ampicillin, 0.008 mg/L of cefotaxime, 0.002 mg/L of ceftriaxone (0.002 mg/L) or
129 no antibiotic (1st passage) (Supplementary Figure S1).

130 The evolving 2-mL cultures were grown in 12-well microtiter plates at 37°C, 100 rpm and 5% CO_2 for
131 four days per cycle, with daily 100-fold dilution into 2 mL of fresh HTM. At each passage, one culture
132 was grown at the same antibiotic concentration as in the previous passage (back-up culture), while
133 three additional cultures were inoculated containing twice the antibiotic concentration of the
134 previous passage. Whenever at least one of the cultures with higher antibiotic concentration showed
135 visible growth after 24 h, this culture was used to inoculate the next passage. This approach allowed
136 for a stepwise increase in antibiotic concentration throughout the experiment without extinction.
137 The highest antibiotic concentration that supported visible growth after 20 passages was recorded as
138 the final concentration: 1 mg/L for ampicillin, 0.125 mg/L for cefotaxime, and 0.064 mg/L for
139 ceftriaxone. At the end of each four-day cycle, 20 µL of culture were spotted onto chocolate agar and
140 incubated for three days at 37°C and 5% CO_2. After incubation, the biomass of the spotted cultures
141 was resuspended in 1 mL of HTM, and 20 µL of this resuspension were used to initiate the next cycle.
142 This process was repeated for a total of five cycles adding up to twenty passages in liquid medium. In
143 the final cycle, cultures were not spotted onto chocolate agar but directly processed. Glycerol stocks
144 (HTM with 20% glycerol) of each passage were stored at -80°C.

145 Single clones were isolated from each passage by dilution streaking of the respective glycerol stocks
146 on chocolate agar. In general, two clones were isolated per passage. However, whenever the
147 antibiotic concentration was increased compared to the previous passage, five clones were isolated
148 instead. Isolated clones were grown in 3 mL of HTM to determine MICs of ampicillin, cefotaxime, and
149 ceftriaxone using gradient diffusion strips (Liofilchem® MIC Test Strips) and to isolate DNA using the
150 DNeasy UltraClean Microbial Kit (Qiagen) for DNA sequencing.

151 Whole genome sequencing

152 Short-read DNA-libraries were prepared from extracted genomic DNA with a modified Illumina
153 Nextera XT library kit protocol as described previously (18). Libraries were sequenced with 150 bp
154 paired-end reads on an Illumina NextSeq 2000 (Illumina, San Diego, CA, USA). Short-read data (fastq
155 files) are available in the European Nucleotide Archieve (ENA) under the BioProject PRJEB86018.
156 Accession numbers are available in Supplementary Table S1. Mutations, i.e., single nucleotide
157 polymorphisms (SNPs), short insertions and deletions, were called with a reference mapping pipeline

158 (19). Briefly, short reads were mapped to the reference genome *H. influenzae* Rd KW20 (ATCC 51907)
159 (BioSample SAMN39831887) using the Burrows-Wheeler Aligner (BWA) (20) and allele calling was
160 done with the Genome Analysis Toolkit (GATK) (21). Mutations were called with the following
161 thresholds: 4 reads mapped in both forward and reverse orientation, a minimum of 8 reads with a
162 PHRED score ≥20 and ≥75% allele frequency. Indels in the gene *hdsM* (i.e., repetitive region) were
163 excluded. For subsequent phylogenetic analysis, SNPs were concatenated when at least 95% of all
164 isolates fulfilled the abovementioned thresholds for read coverage, PHRED score and frequency at
165 individual genome positions.

166 Long-read sequencing was performed with the PacBio Sequel II system (Pacific Biosciences, CA, USA)
167 for selected clones at different timepoints from each evolution experiment to identify structural
168 genomic changes. DNA libraries were prepared with the SMRTbell Express Template Prep Kit 2.0 with
169 barcoded adapters from IDT (Integrated DNA Technologies, USA). Alignment files (.bam) are available
170 in the ENA under the BioProject PRJEB86018. De-novo genome assembly was performed using the
171 PacBio SMRTlink software v9.0 and its "Microbial Assembly" application, with the genome length set
172 to 1.8 Mb and a seed coverage of 30. For the resulting assemblies, the same origin was set using the
173 first 50 bp of dnaA. This sequence was identified using the Seqkit toolkit (Seqkit v2.9.0), and the
174 origin was adjusted accordingly. Subsequently, each assembly was aligned to the reference genome
175 using progressiveMauve (Mauve v2.4.0), and the detected variations were extracted from the
176 alignment. Indels of at least four bases in length were further examined through visual inspection of
177 the assembly and reference mapping in these regions to characterize the mutation more precisely
178 (tandem repeat variation, inversion, deletion, insertion).

179 Long-read sequencing detected deletions and inversions in *ompP2*, which were not detected using
180 Illumina sequencing. To check for presence of structural changes affecting *ompP2* the BWA
181 alignment files of all 315 clones were checked manually for variations in *ompP2* using Geneious
182 Prime v2024.0.5 (https://www.geneious.com/).

183 Phylogenetic and Bayesian analysis

184 Fasttree v.2.1.9 (22) was used to calculate phylogenetic trees for each evolution experiment with a
185 general time reversible (GTR) substitution model and Gamma20 likelihood optimization to account
186 for evolutionary rate heterogeneity among sites and 500 bootstrap replicates. Figtree v.1.4.4
187 (https://github.com/rambaut/figtree/releases) was used to root phylogenetic trees at midpoint and
188 iTol v.6.8.1 (https://itol.embl.de/) was used for visualization. A phylogenetic molecular clock signal
189 was first assessed with TempEst v1.5 (23) by the correlation of sampling day and root-to-tip distance.
190 We further performed a permutation-based linear regression analysis using the lmPerm v2.1.0 R
191 package, to tests the significance of the regression model without assuming normality by computing

p-values through randomized permutations of the data. Mutation rates were calculated with BEAST2.5 (24) for all evolution experiments, except one replicate experiment exposed to ceftriaxone with a poor correlation of SNPs and sampling time, and a non-converging Markov-Chain-Monte-Carlo sampling. We employed a coalescent exponential population model, log normal clock rate, a strict molecular clock, tip dating (day of the experiment), a GTR substitution model, 20 million iterations with 10% burn-in, and sampling every 2,000 traces/trees. Inspection of BEAST log files with Tracer v1.7.2 showed an adequate mixing of the Markov chains and all parameters were observed with an effective sample size (ESS) > 200.

Competitive growth assay

Pairwise competitive growth assays were performed to estimate the *in vitro* relative fitness of mutants evolved in the multi-step evolution experiment compared to the parental strain (*H. influenzae* Rd KW20). Investigated clones were selected to represent a diverse range of mutational patterns. Briefly, five single colonies grown on chocolate agar served as inoculum for 3 mL pre-cultures that were grown until mid-exponential phase (Supplementary Figure S2). Pre-cultures were diluted to an OD_{600} of around 0.025. Equal volumes (1.5 mL) of diluted mutant and parental strain cultures were added in 15 mL falcon tubes. Co-cultures were grown in triplicate for 4 h at 37°C and shaking at 200 rpm. Initial and final colony forming units (CFU) of the mutant and parental strain were determined by standard plate counting on HTM agar (total CFU) and on HTM agar containing 0.016 g/mL cefotaxime (mutant CFU), respectively. Even though co-cultures were inoculated to a 1:1 ratio of the OD_{600} of the two competing strains, initial CFU counts sometimes differed between both strains. Initial CFU ratios of the parental strain to that of the mutant strain of 1:0.5 to 1:2 were accepted, as the formula used below accounts for unequal starting CFUs. Relative fitness was assessed as the ratio of the Malthusian parameter of the mutant to that of the parental (reference) strain. The following formula considering population sizes of the mutant and the parental strain was

$$fitness_{\mathrm{m}} = \frac{\ln\left(\frac{A_{\mathrm{m,\,4h}}}{A_{\mathrm{m,\,0h}}}\right)}{\ln\left(A_{\mathrm{r,\,4h}}\right)}$$

used for the calculation of fitness of each strain in relation to the parental strain (25).

The formula calculates the fitness ($fitness_m$) of the mutant strain relative to the reference strain (Rd KW20). Here, A represents the population size, with subscripts m for the mutant strain and r for the reference strain. The time points 0h and 4h indicate the population size at inoculation and after 4 hours, respectively. A fitness of 1 indicates no fitness cost, whereas a ratio greater than or less than 1 indicates increased or decreased fitness compared to the parental strain, respectively.

Crystal structures

The crystal structure of the transpeptidase domain (amino acid 254-610) of PBP3 of *H. influenzae* was obtained from the RCSB Protein Data Bank (entry ID 6HZO deposited by Bellini et al.). Detected PBP3 substitutions were visualized in this crystal structure using PyMOL v3.0 (https://www.pymol.org/). Ampicillin and cefotaxime were superimposed using crystal structures of PBP3 of *Mycobacterium tuberculosis* (entry ID 6KGW) and *Staphylococcus aureus* (entry ID 3VSL). Structure of full PBP3 (entry ID AF-P45059-F1-v4) was obtained from AlphaFold Protein Structure Database.

AlphaFold Server powered by AlphaFold 3 (26) was used to predict structures of wild-type and mutated Outer membrane protein P2 (OmpP2). Predicted structures were visualized using PyMOL v3.0.

Statistical analyses

The association between specific mutations and a reduction in susceptibility was analyzed using Mann-Whitney U tests. For this purpose, the ampicillin, cefotaxime, and ceftriaxone MIC values of two sets of evolved clones were compared. The clones in the two sets differed genetically only by the mutation or mutation combination under investigation (based on short-read sequencing approach and the manual check of *ompP2* mutations in the BWA alignments), aside from detected tandem repeat variations in the *hsdM* gene. For each clone set, a minimum of three genetically identical clones was required. To minimize the risk of false-positive results due to multiple testing, *p*-values were adjusted using the Benjamini-Hochberg correction. Given that all clones were derived from the same ancestral strain, we acknowledge the possibility of non-independence among observations and interpreted statistical outcomes with caution.

A one-sample t-test (considering the Malthusian parameters $\ln(A_{m,\ 4h}/A_{m,\ 0h})$ and $\ln(A_{r,\ 4h}/A_{r,\ 0h})$) with Benjamini-Hochberg correction for multiple testing was used to assess the significance of fitness gain/loss of mutants compared to the reference strain. Pairwise t-tests with Benjamini-Hochberg correction were conducted to identify significant differences between fitness values of clones isolated from the same evolving population.

A permutation test was conducted to evaluate the association between average fitness and antimicrobial susceptibility (MIC) to ampicillin, cefotaxime, and ceftriaxone. For each antibiotic, the

observed correlation between relative fitness value and MIC was calculated. The null distribution was generated by randomly shuffling the MIC values within each group and recalculating the correlation for 10,000 permutations. The *p*-value was determined by comparing the observed correlation to the null distribution, assessing the statistical significance of the observed association.

Results

Evolution of beta-lactam resistance is mainly driven by *ftsI* and *ompP2* mutations

We exposed the reference strain *H. influenzae* Rd KW20 in a multi-step evolution experiment to increasing concentrations of the three beta-lactam antibiotics ampicillin, cefotaxime, and ceftriaxone. Bacterial populations evolved over 20 transfers in individual experiments, which is equivalent to approximately 200 generations. Overall, we investigated the genomes and MICs of 315 clones, isolated across time from six independent evolution experiments including a drug-free control and three replicate experiments with ceftriaxone. We identified between 11 and 25 mutations (including SNPs and indels) in individual experiments over 20 days of exponential growth, resulting in a linear increase in the number of mutations across time. SNP-based phylogenies and root-to-tip linear regressions (R2 0.31-0.86) indicated moderate to strong support of a constant molecular clock in all evolution experiments, except for one replicate exposed to ceftriaxone (R2 = 0.11) (Supplementary Table S3). Based on a Bayesian coalescent model, assuming a strict molecular clock and exponential population growth, the mutation rates ranged from 1.0×10^{-7} to 2.1×10^{-7} substitutions per site per day.

The MICs against the three beta-lactam antibiotics of individual clones did not change significantly in the drug-free control experiment (Supplementary Figure S3). In the drug-free control, measured MIC differences were within the range of technical variation, i.e., one doubling dilution compared to the MICs of the parental strain Rd KW20, which were 0.19 mg/L for ampicillin, 0.008 mg/L for cefotaxime, and 0.003 mg/L for ceftriaxone. We also did not detect any mutations in the main drug target *ftsI* in the evolved control population (Supplementary Table S1).

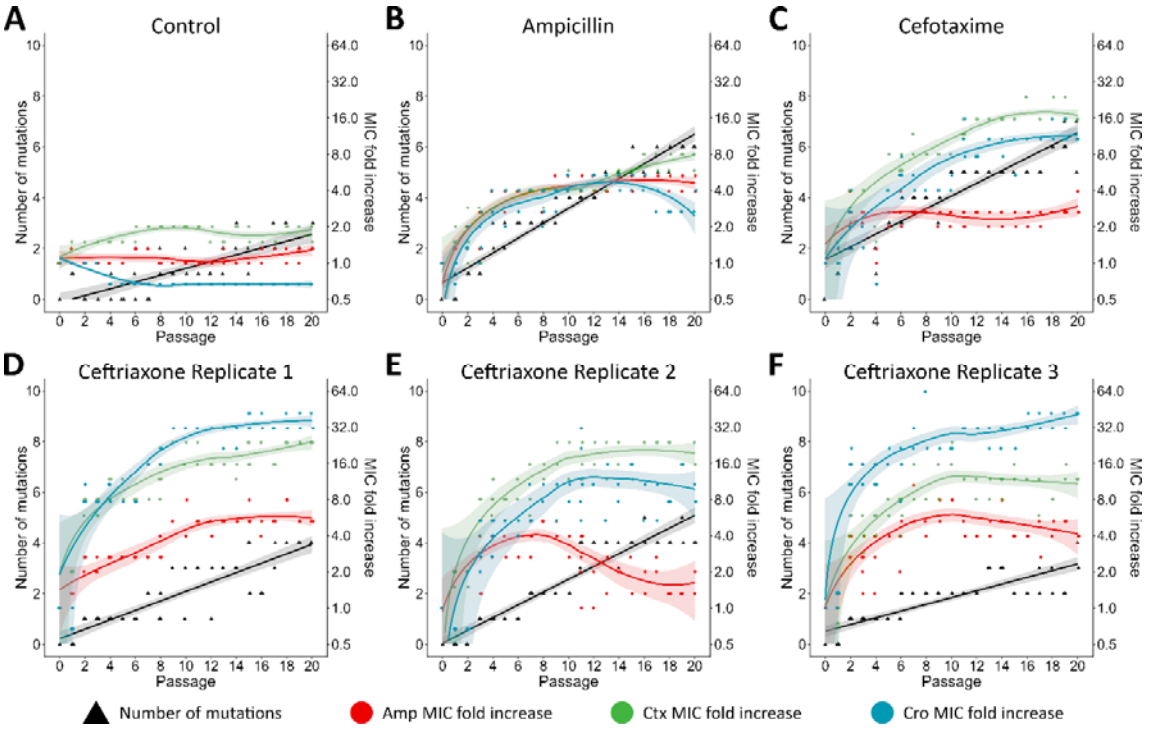

Figure 1: Increasing number of mutations and changes of beta-lactam MICs in six evolution experiments. Number of mutations (black) and minimum inhibitory concentration fold-increase compared to the parental strain Rd KW20 for ampicillin (Amp, red), cefotaxime (Ctx, green), and ceftriaxone (Cro, blue) in selected clones over 20 passages (two or five clones per passage). Bacterial population A - without antibiotic exposure and exposed to increasing concentrations of B - ampicillin, C - cefotaxime, D - ceftriaxone replicate 1, E - ceftriaxone replicate 2, F - ceftriaxone replicate 3. Shaded areas represent the 95% confidence interval.

282 In contrast, exposure to ampicillin, cefotaxime and ceftriaxone resulted in a pronounced increase of
283 beta-lactam MICs (Figure 1). Specifically, exposure to ceftriaxone led to strong MIC increases,
284 including in one clone an MIC increase of up to 64-fold against ceftriaxone relative to the ancestor
285 strain. Exposure to ampicillin resulted in more moderate MIC increases against all three beta-lactam
286 antibiotics. Furthermore, populations exposed to third-generation cephalosporins showed a more
287 pronounced MIC increase against ceftriaxone and cefotaxime as compared to ampicillin.

288 Clinical resistance against cefotaxime (EUCAST breakpoint: > 0.125 mg/L) was observed for 4/55
289 (7.3%) clones evolved under cefotaxime exposure and for 28/169 (16.6%) clones evolved in three
290 evolution experiments under ceftriaxone exposure (Figure 2, Supplementary Figure S3). Exposure to
291 ceftriaxone further selected 1/169, (0.6%) ceftriaxone resistant (EUCAST breakpoint: > 0.125 mg/L)
292 clone and 10/169 (5.9%) ampicillin resistant (EUCAST breakpoint: > 1 mg/L) clones. Cross-resistance
293 against ampicillin and cefotaxime was observed for five clones evolved under ceftriaxone exposure
294 (Supplementary Figure S3). Overall, 20 days exposure to ampicillin did not select for clinical resistant
295 clones against any of the three tested drugs.

296 As expected, increasing MICs against the beta-lactam antibiotics were associated with mutations in
297 *ftsI* (Figure 2, Supplementary Figure S3). Out of 136 evolved clones that exhibited at least one *ftsI*
298 mutation, 18 were resistant according to EUCAST breakpoints for cefotaxime, but none were
299 resistant to ampicillin or ceftriaxone. Specifically, we identified combinations of the following five
300 amino acid (amino acid) substitutions in individual clones in the transpeptidase domain: p.Thr332Ile
301 (c.968C>T), p.Thr443Ala (c.1327A>G), p.Ala530Ser (c.1591G>T), p.Asp551Tyr (c.1652G>T), and
302 p.Ala561Glu (c.1684C>A). Exposure to both ampicillin and cefotaxime, selected for p.Ala530Ser.
303 Under cefotaxime conditions p.Ala530Ser, p.Thr443Ala, and p.Thr332Ile evolved in a stepwise
304 manner. The substitutions p.Asp551Tyr and p.Ala561Glu were detected independently in separate
305 clones, each arising contemporaneously (detected in 3rd passage) in one population exposed to
306 ceftriaxone. The detected *ftsI* mutations were significantly associated with MIC increase of beta-
307 lactams (Supplementary Table S4). In a crystal structure model of PBP3, all five *ftsI* mutations were
308 either in proximity to other well-known resistance-associated amino acid positions (Ile449, Arg517,
309 Asn526), or close to the binding site of the antibiotics (Figure 3).

310

Figure 2: Maximum likelihood phylogeny of *H. influenzae* Rd KW20 clones evolved in the presence of ampicillin (A, 53 clones), cefotaxime (B, 56 clones), and ceftriaxone (C, 57 clones). Amino acid substitutions in the penicillin binding protein 3 (PBP3) and presence of mutations in specified genes as well as minimum inhibitory concentration (MIC) changes over time are color coded. Strains that exceeded the clinical breakpoint for ampicillin/cefotaxime/ceftriaxone according to EUCAST breakpoints are marked with a white star at the MIC heatmap.
The specified genes are those in which at least 20 clones from the whole set of selected clones exhibited mutations but did not mutate under antibiotic-free conditions.

312 Furthermore, *ftsI* mutations differentially affected the susceptibility against ampicillin, cefotaxime,
313 and ceftriaxone. While we observed a significant MIC increase for ampicillin (2-fold increase, p_{adj} =
314 0.008) and ceftriaxone (3-fold increase, p_{adj} = 0.004) associated with amino acid substitution
315 p.Ala530Ser, the secondary amino acid substitution p.Thr443Ala did not significantly affect ampicillin
316 susceptibility but was associated with a two-fold increase of the MIC towards cefotaxime (p_{adj} =
317 0.019) (Supplementary Table S4). Out of the five detected PBP3 substitutions, p.Asp551Tyr showed
318 the highest MIC fold increase towards all three beta-lactams with a maximum 8-fold increase of the

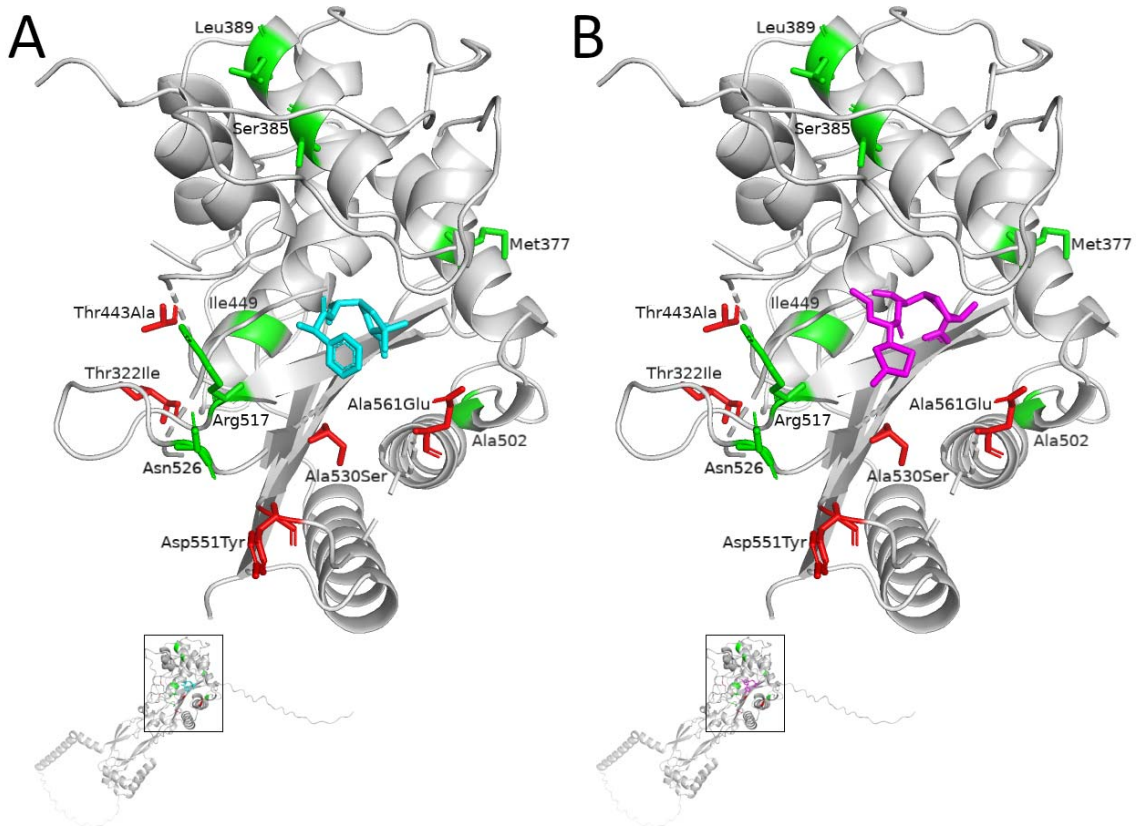

Figure 3: Crystal structure of transpeptidase domain (residues 254-610) of the penicillin binding protein 3 (PBP3) of *H. influenzae* (Bellini et al. [2019]) with superimposed ampicillin (A, colored in cyan) and cefotaxime (B, colored in magenta) molecules. *In vitro* selected amino acid substitutions in PBP3 Thr332Ile, Thr443Ala, Ala530Ser, Asp551Tyr, and Ala561Glu are colored in red. Known positions for amino acid substitutions defining established PBP3 resistance groups are colored in green.

319 MIC of ceftriaxone (p_{adj} = 2E-06).

320 Surprisingly, clones isolated from populations exposed to ceftriaxone (replicate 1 and replicate 3) did
321 not harbor any mutations in *ftsI*. However, we repeatedly selected different mutations in the *outer*
322 *membrane protein P2 (ompP2)*, i.e., p.Thr126fs (c.376_377insT), p.Val353fs (g.902541_902708del), as
323 well as a structural re-arrangement comprising a genomic inversion starting at codon 353 resulting in
324 p.Gly354fs (g.902541_902708inv). The latter two mutations were not detected with the short-read

325 reference mapping approach but were identified based on the long-read assemblies. However, both
326 mutations could also be detected in clones, for which no long-read sequencing data were available,
327 through a manual check of the BWA alignments. In addition, various tandem repeat variations in
328 different genes could be detected using the long-read sequencing data (Supplementary Table S2).
329 Mutation p.Thr126fs introduces a stop codon at position 129 in *ompP2*, resulting in a truncated
330 protein of only 128 amino acids instead of 359 amino acids (Supplementary Figure S4). The other two
331 mutations starting at codon 353 (i.e., g.902541_902708inv and g.902541_902708del) affect the C-
332 terminus of OmpP2, specifically the last β-strand of the β-barrel (Supplementary Figure S5). The
333 mutation g.902541_902708inv evolved independently in two replicate experiments. All three *ompP2*
334 mutations were significantly (p_{adj} < 4E-05) associated with a MIC increase against all three beta-
335 lactam antibiotics with a more pronounced effect for ceftriaxone susceptibility (i.e., 11.5-fold MIC
336 increase, as compared to 2-fold and 3.9-fold increase for ampicillin and cefotaxime, respectively).
337 Overall, 104/315 evolved clones carried ompP2 mutations, of which 10 were resistant to ampicillin,
338 14 to cefotaxime, and one to ceftriaxone according to EUCAST breakpoints. However, all resistant
339 clones with *ompP2* mutations harbored additional mutations, for example, in the *pnp* gene. Clones
340 with *ompP2* mutations only exhibited highly increased MICs, but these were below the respective
341 EUCAST clinical breakpoints (Supplementary Table S4).

342 Interestingly, strains harboring the inversion mutation (g.902541_902708inv) resulting in p.Gly354fs
343 were phenotypically heterogeneous concerning beta-lactam susceptibility. Respective strains showed
344 two ellipses for all three beta-lactams on the agar plates with gradient diffusion strips
345 (Supplementary Figure S6). The lower MIC corresponded to the MIC observed for the parental strain
346 ± two doubling dilutions.

347 Besides mutations in *ftsI* and *ompP2*, we detected 13 different mutations in *pnp* (encoding
348 polyribonucleotide nucleotidyltransferase) in clones with and without pre-existing *ftsI* or *ompP2*
349 mutations isolated from populations exposed to cefotaxime, and in two replicated experiments
350 under ceftriaxone. Of those 13 mutations, seven induced a premature stop codon (p.Glu18*,
351 p.Lys47*, p.Glu80*, p.Gln159*, p.Glu220*, p.Glu471*, p.Met601*), three resulted in a frameshift
352 (p.Val423fs, p.Gly444fs, p.Glu580fs) and three were non-synonymous SNPs (p.Ala440Val,
353 p.Gln505Lys, p.Gly626Cys). p.Glu220* and p.Glu580fs were associated with a significant (p_{adj} < 0.034)
354 MIC increase for all three beta-lactams in clones with p.Thr126fs in OmpP2 (Supplementary Table
355 S4). The effect of the other detected mutations in *pnp* could not be determined due to an insufficient
356 number of clones carrying the specific mutation pattern. Four different mutations in *rpoB* (encoding
357 DNA-directed RNA polymerase subunit beta), three of them in close proximity (p.Leu149Phe,
358 p.Arg151His, p.Gly154Asp), were detected in clones isolated from populations exposed to ampicillin

and ceftriaxone (replicate 2). Furthermore, clones derived from ampicillin, cefotaxime, and ceftriaxone (replicate 2) exposed populations evolved four different mutations in *udk* (encoding uridine kinase) and *spoT* (encoding Guanosine-3',5'-bis(diphosphate) 3'-pyrophosphohydrolase). Two mutations in *prs* (encoding ribose-phosphate pyrophosphokinase) were detected in ampicillin exposed clones as well as two mutations in Rd_08000 (encoding a putative TonB-dependent receptor) in ceftriaxone exposed clones (replicate 1 and 3). However, only minor effects were observed, with a maximum median MIC fold increase of 3 for mutations in genes other than *ftsI* and *ompP2*.

Evolved resistant mutants pay a fitness cost under drug-free conditions

368 To investigate possible fitness costs of specific mutants and identify putative compensatory

369 mutations that minimize the fitness costs imposed by resistance-associated mutations, a competitive

370 growth assay was performed. Most of the evolved clones exhibited a lower fitness compared to the

371 parental strain (Figure 4 and Supplementary Table S1), strongly indicating an evolutionary trade-off

372 between resistance and competitive fitness in the absence of antibiotics. However, three strains

373 (E_0.5Amp_07a, E_1Amp_17a and E_0.032Ctx_07a) did not show a fitness/growth defect. One of

these clones (E_0.5Amp_07a) harbored putative beta-lactam susceptibility decreasing mutations in

375 *ftsI* and *rpoB* (27–29) accompanied by a mutation in *udk*. Another clone (E_1Amp_17a) showed the

same mutation pattern but with additional mutations in *rpoA*, *plsB*, and *prs*.

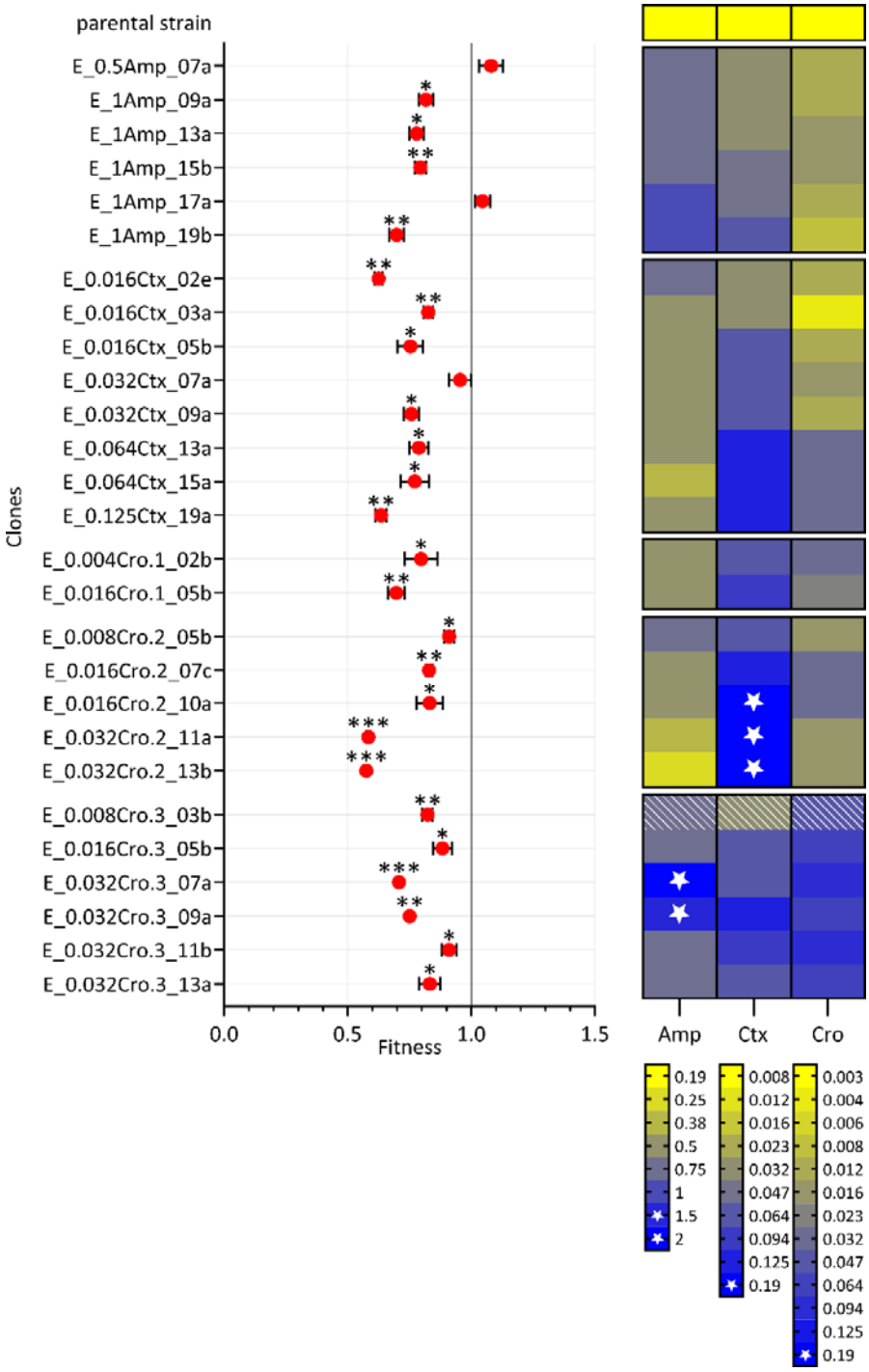

Figure 4: Bacterial fitness of selected clones derived from evolving populations exposed to ampicillin, cefotaxime, and ceftriaxone. Bacterial fitness measured as relative growth difference between the ancestral strain (*H. influenzae* Rd KW20) and the selected clone. A relative fitness of 1 indicates no fitness cost, whereas a value greater or less than 1 indicates increased or decreased fitness, respectively. The black bars represent standard deviation. $*p_{adj} < 0.05$; $**p_{adj} < 0.01$; $***p_{adj} < 0.001$. The heatmap indicates MIC values of ampicillin (Amp), cefotaxime (Ctx) and ceftriaxone (Cro) in mg/L of the respective strain (already presented in Figure 2). Stars indicate clinical resistance above the respective EUCAST breakpoints. Hatched panels indicate phenotypic heterogeneity. Clones that derived from the same evolution experiment are grouped together on the y-axis.

Pairwise t-tests were conducted to compare all clones from a given evolution experiment. Particularly interesting are comparisons between clones that differ by only a single mutation, as these allow for the evaluation of fitness effects of individual mutations within a specific genetic background. Comparison of fitness assay results of E_1Amp_17a and E_1Amp_13a revealed, that the *rpoA* mutation restored wild-type fitness level in the respective mutational background (Supplementary Table S5). Clone E_0.032Ctx_07a exhibits putative beta-lactam susceptibility decreasing mutations in *ftsI* and *pnp* (30,31) accompanied by mutated *plsB*. In this case, comparison with fitness assay results of E_0.016Ctx_05b, revealed that evolution of the *plsB* mutation resulted in wild-type fitness in the respective mutational background. Moreover, fitness decrease could directly be addressed to and quantified for specific mutations in *ftsI* (p.Asp551Tyr), *ompP2* (p.Thr126fs, p.Val353fs), and *pnp* (p.Glu580fs, p.Glu220*). Correlating MIC increases and relative fitness of evolved clones revealed a negative correlation between MIC and fitness for cefotaxime (coefficient = -0.45, p = 0.019), but no correlation of MICs and fitness for ampicillin and ceftriaxone (Supplementary Table S6).

Evolved beta-lactam resistance is commonly associated with collateral sensitivity towards aminoglycosides, clarithromycin, vancomycin, and colistin

To assess the expression of collateral effects, we characterized resistance to 14 antibiotics from different classes for 17 clones isolated from the evolution experiments. We identified a consistent pattern of decreased susceptibility for beta-lactam antibiotics (Figure 5). This also includes increased MICs of the carbapenem meropenem. In this case, two clones (E_1Amp_10b and E_1Amp_19b) with increased MICs of ampicillin, cefotaxime, and ceftriaxone expressed cross-resistance to meropenem at above EUCAST breakpoint levels. Surprisingly, two clones evolved under ceftriaxone exposure exhibited increased susceptibility (i.e., collateral sensitivity) to meropenem. These two clones additionally showed collateral sensitivity towards all non-beta-lactam antibiotics, excluding tetracycline. In general, collateral sensitivity is most often expressed towards the three considered aminoglycoside drugs (amikacin, kanamycin, and gentamicin), towards the macrolide clarithromycin, as well as the polymyxin drug colistin, possibly indicating a robust emergence of collateral sensitivity upon beta-lactam resistance evolution in *H. influenzae*.

Moreover, the two identified phenotypically heterogeneous OmpP2 mutants consistently expressed phenotypical heterogeneity (i.e., two ellipses with a gradient diffusion test) towards a variety of antibiotics, including next to the beta-lactams also fluoroquinolones, rifampicin and, tetracycline.

410

411

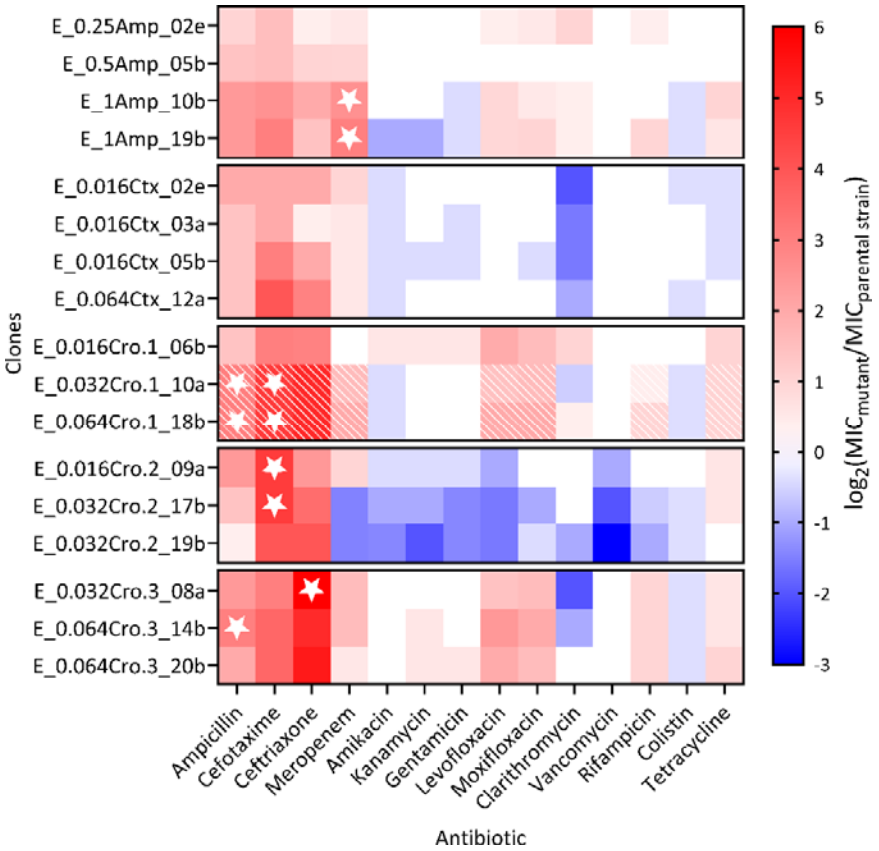

Figure 5: Collateral effects of increased MICs against individual beta-lactam antibiotics. Heat map of log_2-transformed relative increase in MIC of ampicillin, cefotaxime, ceftriaxone (underlying MIC values already presented in Figure 1), meropenem (beta-lactams), amikacin, kanamycin, gentamicin (aminoglycosides), levofloxacin, moxifloxacin (fluoroquinolones), clarithromycin (macrolide), vancomycin (glycopeptide), rifampicin (ansamycin), colistin (polymyxin) and tetracycline (tetracycline) in mutant clones relative to the MIC of the parental strain *H. influenzae* Rd KW20. Selected clones were evolved in the multi-step evolution experiment. Stars indicate clinical resistance above the respective EUCAST breakpoints (not available for aminoglycosides, clarithromycin, vancomycin, and colistin). Hatched panels indicate phenotypic heterogeneity. Clones that derived from the same evolution experiment are grouped together on the y-axis.

Discussion

This study characterizes the *in vitro* evolution of resistance against three clinically relevant beta-lactam antimicrobials in the opportunistic human pathogen *H. influenzae*. Our results revealed an approximately linear increase in the number of mutations across time, while susceptibility against the antibiotics decreased more steeply during early passages and tended to plateau in the later passages, with dynamics varying across the different beta-lactams and replicates. These increases in resistance are mainly mediated by mutations in previously characterized AMR genes and, in two populations, is additionally associated with the emergence of phenotypic heterogeneity. Generally, evolved resistance against one antibiotic caused significant fitness reductions in drug-free environments and led to altered phenotypic responses to other drug classes, including numerous cases of collateral sensitivity, especially towards aminoglycosides and additional drug classes. Understanding evolutionary pathways and predicting their impact on future treatment regimens will be crucial to reduce bacterial adaptation and selection of antimicrobial resistances.

Respiratory infections with *H. influenzae* are usually treated with an aminopenicillin in combination with a beta-lactamase inhibitor (to overcome beta-lactamase-mediated resistance). In case of treatment failure or for severe invasive infections such as sepsis or meningitis, the use of third-generation cephalosporins such as cefotaxime and ceftriaxone is endorsed. However, it is still unclear whether cephalosporin resistance can also develop through alternative evolutionary pathways beyond the well-known PBP3 group III mutations. Furthermore, while resistance to ceftriaxone and cefotaxime is currently rare in clinical isolates (32), understanding potential evolutionary pathways to resistance and collateral effects is crucial for anticipating future threats and optimizing treatment strategies.

To address this, we performed *in vitro* evolution experiments by exposing *H. influenzae* Rd KW20 to increasing concentrations of ampicillin, cefotaxime, and ceftriaxone and monitored genomic changes. Except for p.Thr322Ile, all PBP3 substitutions that were identified in these experiments, were previously reported (in combination with other amino acid substitutions) for patient-derived isolates, and exhibiting decreased susceptibility to cephalosporins and/or ampicillin (p.Thr443Ala (34–37), p.Ala530Ser (34,35,37–40), p.Asp551Tyr (34) and p.Ala561Glu (39)). Notably, none of the PBP3 ampicillin resistance group-defining mutations (p.Met377Ile, p.Ser385Thr, p.Leu389Phe, p.Ile449Val, p.Ala502Val/Thr, p.Arg517His and p.Asn526Lys) evolved in the evolution experiments, although p.Arg517His and p.Asn526Lys are two well-known driver mutations for ampicillin and cefotaxime resistance (41,42). However, PBP3 p.Thr322Ile and p.Thr443Ala, that evolved under cefotaxime exposure, are in close spatial proximity of Asn526 and Arg517, respectively. Interestingly, the resulting structural changes in the beta-lactam binding site of PBP3, seem to mainly affect

446 resistance to cephalosporins rather than ampicillin. In *in vitro* evolution experiments with NTHi
447 performed by Jakubu et al.(43), one strain with wild-type *ftsI* evolved p.Thr443Ala in the presence of
448 the cephalosporine cefuroxime. In accordance with our results, the respective population showed
449 only a MIC increase for the cephalosporine, but not ampicillin. Hence, cephalosporins can select for
450 amino acid substitutions that do not affect ampicillin susceptibility.

451 However, we also observed convergent evolution of p.Ala530Ser under both ampicillin and
452 cefotaxime selection pressure. Respective clones showed significantly increased MICs especially of
453 ampicillin and ceftriaxone demonstrating that amino acid substitution in PBP3 can show collateral
454 effects for beta-lactam antibiotics. Further studies, that elucidate to what extent specific *ftsI*
455 mutations and mutation patterns affect third-generation cephalosporin susceptibility as well as
456 information on treatment outcome are essential to evaluate this and improve clinical decision
457 making.

458 Interestingly, we also observed clones with highly increased beta-lactam MICs that did not harbor
459 any *ftsI* mutations. Ceftriaxone exposure led to evolution of three different *ompP2* mutations
460 resulting in a profound effect on MICs of all three beta-lactam antibiotics. OmpP2 is one of the major
461 outer membrane proteins in *H. influenzae* with a mass of approximately 36 to 42 kDa. The protein
462 functions as a porin with an exclusion limit of about 1.4 kDa (44,45). Studies analyzing the *ompP2*
463 gene of *H. influenzae* reported a high conservation of the 16 β-strands building up the β-barrel, but
464 increased variation and accumulation of SNPs in the eight surface-exposed loop regions (46–49),
465 which can result in antigenic variation (50,51). By expression of OmpP2 and the AcrAB (multidrug
466 efflux pump) encoding genes of *H. influenzae* in an *acrB* and *ompF* knockout strain of *Escherichia coli*,
467 Zwarma et al. provided evidence that sensitivity to beta-lactams in *H. influenzae* actually is affected
468 by OmpP2. While the efflux pump AcrAB-TolC actively transports antibiotics from the cytoplasm and
469 periplasm out of the cell, OmpP2 counterbalances this efflux by leaking the drugs back into the cell
470 (52).

471 Our findings confirm that diverse mutations in *ompP2* can significantly contribute to highly increased
472 beta-lactam MICs in *H. influenzae* (49,53,54). These *ompP2* mutations seem to be particularly
473 selected under ceftriaxone exposure. The *ompP2* frameshift mutation p.Thr126fs detected in this
474 study resulted in a stop codon at amino acid position 129 (instead of position 361) and therefore
475 probably generated a non-functional protein. The other two mutations resulting in p.Val353fs
476 (deletion) and p.Gly354fs (inversion) affected only the last β-strand of the porin, though AlphaFold
477 predicted the mutated sequence to not alter the β-barrel structure. Therefore, decreased influx of
478 beta-lactam antibiotics might have resulted from an altered electrostatic profile within the porin
479 channel due to residue properties of the changed AAs (55–57). Most studies on beta-lactam

480 resistance in *H. influenzae* focus on PBP3, which makes evaluation of the clinical relevance of *ompP2*
481 mutations and their contribution to treatment failure difficult.

482 Additional genes, with possibly more moderate effects on ampicillin, cefotaxime, and/or ceftriaxone
483 susceptibility are *rpoB*, *pnp*, and *spoT*. Mutations in these three genes have already been associated
484 with antibiotic resistance in other studies (58) or were selected in comparable evolution experiments
485 with *H. influenzae* (43,54), *E. coli* (59), and *Staphylococcus aureus* (60). RNA polymerase subunit β is
486 essential for transcription and even though specific mutations in *rpoB* are known to cause rifampicin
487 resistance, the gene was also recently associated with beta-lactam susceptibility in *Neisseria*
488 *gonorrhoeae* (27), *S. aureus* (27), and *Bacillus subtilis* (29). The highly conserved PNPase, which
489 influences mRNA and small RNA stability, is described to affect resistance and tolerance to
490 ciprofloxacin and aminoglycosides in *Pseudomonas aeruginosa*, respectively (30,31). The
491 pyrophosphohydrolase encoded by *spoT* synthesizes and hydrolyzes alarmone ppGpp, which induces
492 the expression of stress resistance components, and is involved in resistance and tolerance against
493 different antibiotics including beta-lactams for example in *P. aeruginosa* and *Helicobacter pylori* (61–
494 63). In our study, the effect of mutations in *rpoB, pnp and spoT* genes was limited to a two-fold MIC
495 increase. Therefore, one of the detected mutations alone does not result in beta-lactam resistance.
496 However, these novel association with decreased beta-lactam susceptibility in *H. influenzae* highlight
497 the complex interplay of various genetic factors in resistance mechanisms.

498 Drug resistance mutations often entail a reduced fitness in the absence of antibiotic pressure (64,65)
499 as the antibiotic target is often involved in important cellular processes (66). Indeed, almost all of the
500 clones examined exhibited a significant fitness deficit, with significant variability across mutants.
501 Notably, mutations associated with a higher increase in MIC do not necessarily entail a greater
502 fitness deficit. This is exemplified by the amino acid substitution p.Asp551Tyr in PBP3, which resulted
503 in only a moderate fitness decrease of approximately 9% (within the wild-type genomic background)
504 but was associated with an 8-fold increase of the MIC of ceftriaxone. Fitness levels can influence the
505 evolutionary success of a mutant. It is assumed that mutants with little or no fitness deficit tend to
506 be more successful (67). This is supported by studies on *Mycobacterium tuberculosis* and
507 *Staphylococcus aureus*, which discovered mutations with the lowest fitness costs to be the ones most
508 frequently identified in resistant clinical isolates (68–70).

509 In addition, the frameshift mutation in *ompP2* was associated with a relatively moderate fitness
510 deficit of approximately 12%. At the same time, this mutation provided a significant advantage in the
511 presence of the antibiotic, with a 23.5-fold increase in the MIC of ceftriaxone. In the evolution
512 experiment, the *ompP2* frameshift mutations outcompeted the inversion mutant over time, as both
513 mutations were initially detected in the second passage, but just the frameshift mutation persisted

514 until passage 20. However, applied bottlenecks, such as the 1:100 dilution used for passaging in this
515 study, inherently impose a random selection, as only a small, randomly chosen subset of the growing
516 population can proliferate in the next passage, thus increasing the effect of genetic drift. Genetic
517 drift influences the manifestation of specific mutations, as certain variants may be lost or
518 disproportionately represented purely by chance (71–73). A specificity of OmpP2 for NAD as well as
519 highly reduced uptake of NAD in *ompP2* knockout strains has been described for *H. influenzae* (74).
520 This might explain the reduced fitness observed for clones with mutated *ompP2*, as *H. influenzae* is
521 dependent on extracellular NAD (75) due to the lack of enzymes necessary for de novo biosynthesis
522 (76).

523 In cases of entailed fitness costs, fitness can be restored by reverting the resistance causing
524 mutation, which is just possible in the absence of antibiotic pressure (77), and by the acquisition of
525 compensatory mutations (64). We identified that the p.Thr443Ala substitution in PBP3 mitigates the
526 fitness deficit caused by p.Ala530Ser in PBP3 (and p.Val423fs in *pnp*), while this amino acid
527 substitution is also associated with a slight increase in the MIC of third-generation cephalosporins.
528 Such mutations likely present an increased risk for being selected in the presence and the absence of
529 the antibiotic.

530 Resistance-conferring mutations can additionally affect susceptibility to other antibiotics.
531 Simultaneously acquired resistance to another antibiotic is referred to as cross-resistance, while
532 collateral sensitivity describes an evolutionary trade-off where antibiotic resistance to one antibiotic
533 confers increased susceptibility to another antibiotic. Robust collateral sensitivity phenotypes could
534 help to develop new evolutionary-based treatment strategies and therefore may reduce resistance
535 emergence (78).

536 We observed collaterally increased MICs of fluoroquinolones in *ompP2* mutated clones with
537 decreased beta-lactam susceptibility. This influence of OmpP2 on fluoroquinolone susceptibility in *H.*
538 *influenzae* is supported by evolution experiments with clinical isolates of *H. influenzae* in the
539 presence of moxifloxacin that selected for *ompP2* mutations and MICs exceeding CLSI breakpoints for
540 moxifloxacin (54). In our experiments MICs did not exceed EUCAST clinical breakpoints for
541 moxifloxacin (> 0.125 mg/L) and levofloxacin (> 0.06 mg/L). However, the success of treatment with
542 fluoroquinolones might be reduced in these cases. For the macrolide clarithromycin we observed
543 differential effects in the *ompP2* mutants. These observations may be clinically relevant, as *H.*
544 *influenzae* could be treated with co-trimoxazole, macrolides, fluoroquinolones, or tetracycline in
545 cases of known resistance or intolerance to β-lactam antibiotics (79).

546 Overall, our study identified the emergence of collateral sensitivity towards the three tested
547 aminoglycosides, against the macrolide clarithromycin, the glycopeptide vancomycin, and also the

548 polymyxin drug colistin. Especially the reduced MIC to vancomycin in one evolution experiment was
549 surprising as this antibiotic is only active against gram positive bacteria. This effect might be linked to
550 the detected mutation in the *mltC* gene, as increased susceptibility to vancomycin under acidic pH
551 has been observed in a MltC/MltE deletion mutant of *Escherichia coli* (80). Overall, these patterns of
552 evolved collateral sensitivity were observed for more than 50% of the tested clones. Even though
553 they did not emerge in all cases, collateral sensitivities seem to occur frequently towards specific
554 antibiotics and may thus be a promising focus for optimizing antibiotic treatment designs.

555 The therapeutic potential of such evolutionary trade-offs clearly deserves further study, especially
556 using combinatorial and sequential treatments with a beta-lactam and an aminoglycoside or
557 clarithromycin. Unfortunately, due to the ototoxicity and nephrotoxicity, which are common side
558 effects of aminoglycosides, a potential combinatorial or alternating treatment would not be
559 appropriate for simple respiratory tract infections caused by *H. influenzae* (81), but rather of value
560 for severe infections like meningitis or sepsis. In fact, beta-lactam–aminoglycoside combinations are
561 used in cases like neonatal meningitis or severe sepsis of unknown etiology, where *H. influenzae* is
562 only rarely the causative pathogen. Nevertheless, in such cases, according to our findings this therapy
563 could be effective.

564 Limitations

565 *H. influenzae* Rd KW20, a well-characterized reference strain, was used as the starting point for all
566 evolution experiments. This represents a limitation, as evolutionary trajectories and phenotypic
567 effects of mutations may vary by genetic background (33). While our findings offer a valuable
568 foundation, the generalizability of resistance-associated fitness and collateral effects should be
569 confirmed in diverse clinical isolates. Future studies incorporating the detection of resistance
570 mutations identified here will be essential to assess their broader clinical relevance across diverse
571 genetic backgrounds.

572 Conclusion

573 Overall, this study revealed the fast evolution of beta-lactam resistance in the opportunistic human
574 pathogen *H. influenzae*. Evolved resistance is mediated by an accumulation of mutations in known
575 target genes and in two populations associated with the emergence of heterogeneity in
576 susceptibility. Almost all resistant clones suffered from reduced competitive fitness in the absence of
577 antibiotics and often expressed collateral sensitivity towards other drug classes, especially
578 aminoglycosides. These findings indicate robust evolutionary trade-offs that are caused by the
579 resistance-conferring mutations and may represent a promising focus for optimizing antibiotic
580 treatment designs. Similarly, a further analysis of novel resistance mutations and of epistatic effects
581 may additionally assist to improve the development of new antimicrobial treatment strategies.

Acknowledgments

We thank T. Niemann, V. Mohr, M. Mundzeck, T. Struve from the Research Center Borstel, Germany for excellent technical assistance.

Funding

We are grateful for financial support from the German Science Foundation within the Research and Training Group 2501 (RTG 2501) on Translational Evolutionary Research (project 4.2, to HS; and associated doctoral project of SP), the Max-Planck Society (Fellowship to HS), the Deutsche Forschungsgemeinschaft (DFG, German Research Foundation) under Germanys Excellence Strategy – EXC 2167 Precision Medicine in Inflammation, the German Ministry of Education and Research (BMBF) for the German Center of Infection Research (DZIF), and the Leibniz Science Campus Evolutionary Medicine of the LUNG (EvoLUNG).

Transparency Declaration

The authors declare that they do not have any competing interests.

Author contributions

SP, MD and MM conceived the study. SP performed evolutionary experiments, phenotyping and statistical analysis. MM performed Bayesian clock dating analysis. SP, MD, and CU performed next generation sequencing. SP and MM wrote the first draft, all authors reviewed the manuscript, and provided intellectual input. All authors read and approved the final manuscript.

References

1. Antimicrobial Resistance Collaborators. Global burden of bacterial antimicrobial resistance in 2019: a systematic analysis. Lancet Lond Engl. 2022 Feb 12;399(10325):629–55.

2. WHO bacterial priority pathogens list, 2024: Bacterial pathogens of public health importance to guide research, development and strategies to prevent and control antimicrobial resistance [Internet]. [cited 2024 Oct 18]. Available from: https://www.who.int/publications/i/item/9789240093461

3. Clark SE. Commensal bacteria in the upper respiratory tract regulate susceptibility to infection. Curr Opin Immunol. 2020 Oct;66:42–9.

4. Teo SM, Mok D, Pham K, Kusel M, Serralha M, Troy N, et al. The Infant Nasopharyngeal Microbiome Impacts Severity of Lower Respiratory Infection and Risk of Asthma Development. Cell Host Microbe. 2015 May 13;17(5):704–15.

5. Tsang RSW, Ulanova M. The changing epidemiology of invasive *Haemophilus influenzae* disease: Emergence and global presence of serotype a strains that may require a new vaccine for control. Vaccine. 2017 Jul 24;35(33):4270–5.

6. Whittaker R, Economopoulou A, Dias JG, Bancroft E, Ramliden M, Celentano LP. Epidemiology of invasive *Haemophilus influenzae* disease, Europe, 2007–2014. Emerg Infect Dis J. 2017;23(3):396.

617 7. Heinz E. The return of Pfeiffer's bacillus: Rising incidence of ampicillin resistance in *Haemophilus*
618 *influenzae*. Microb Genomics. 2018;4(9).

619 8. Zhou M, Fu P, Fang C, Shang S, Hua C, Jing C, et al. Antimicrobial resistance of *Haemophilus*
620 *influenzae* isolates from pediatric hospitals in Mainland China: Report from the ISPED program,
621 2017–2019. Indian J Med Microbiol. 2021 Oct 1;39(4):434–8.

622 9. Tsang RSW, Shuel M, Whyte K, Hoang L, Tyrrell G, Horsman G, et al. Antibiotic susceptibility and
623 molecular analysis of invasive Haemophilus influenzae in Canada, 2007 to 2014. J Antimicrob
624 Chemother. 2017 May 1;72(5):1314–9.

625 10. Scriver SR, Walmsley SL, Kau CL, Hoban DJ, Brunton J, McGeer A, et al. Determination of
626 antimicrobial susceptibilities of Canadian isolates of *Haemophilus influenzae* and characterization
627 of their beta-lactamases. Antimicrob Agents Chemother. 1994;38(7):1678–80.

628 11. Farrell DJ, Morrissey I, Bakker S, Buckridge S, Felmingham D. Global distribution of TEM-1 and
629 ROB-1 β-lactamases in *Haemophilus influenzae*. J Antimicrob Chemother. 2005;56(4):773–6.

630 12. Red Book (2021): Report of the Committee on Infectious Diseases. American Academy of
631 Pediatrics; 2021.

632 13. Bennett JE, Dolin R, Blaser MJ. Mandell, Douglas, and Bennett's Principles and Practice of
633 Infectious Diseases: 2-Volume Set. Elsevier Health Sciences; 2014. 5094 p.

634 14. Parr TR, Bryan LE. Mechanism of resistance of an ampicillin-resistant, beta-lactamase-negative
635 clinical isolate of *Haemophilus influenzae* type b to beta-lactam antibiotics. Antimicrob Agents
636 Chemother. 1984;25(6):747–53.

637 15. Ubukata K, Shibasaki Y, Yamamoto K, Chiba N, Hasegawa K, Takeuchi Y, et al. Association of
638 amino acid substitutions in penicillin-binding protein 3 with β-lactam resistance in β-lactamase-
639 negative ampicillin-resistant *Haemophilus influenzae*. Antimicrob Agents Chemother.
640 2001;45(6):1693–9.

641 16. Jansen G, Barbosa C, Schulenburg H. Experimental evolution as an efficient tool to dissect
642 adaptive paths to antibiotic resistance. Drug Resist Updat Rev Comment Antimicrob Anticancer
643 Chemother. 2013 Dec;16(6):96–107.

644 17. Batra A, Roemhild R, Rousseau E, Franzenburg S, Niemann S, Schulenburg H. High potency of
645 sequential therapy with only β-lactam antibiotics. eLife. 2021 Jul 28;10:e68876.

646 18. Baym M, Kryazhimskiy S, Lieberman TD, Chung H, Desai MM, Kishony R. Inexpensive multiplexed
647 library preparation for megabase-sized genomes. PloS One. 2015;10(5):e0128036.

648 19. Kohl TA, Utpatel C, Schleusener V, De Filippo MR, Beckert P, Cirillo DM, et al. MTBseq: a
649 comprehensive pipeline for whole genome sequence analysis of Mycobacterium tuberculosis
650 complex isolates. PeerJ. 2018;6:e5895.

651 20. Li H, Durbin R. Fast and accurate short read alignment with Burrows-Wheeler transform.
652 Bioinforma Oxf Engl. 2009 Jul 15;25(14):1754–60.

653 21. McKenna A, Hanna M, Banks E, Sivachenko A, Cibulskis K, Kernytsky A, et al. The Genome
654 Analysis Toolkit: a MapReduce framework for analyzing next-generation DNA sequencing data.
655 Genome Res. 2010 Sep;20(9):1297–303.

656 22. Price MN, Dehal PS, Arkin AP. FastTree 2 – Approximately Maximum-Likelihood Trees for Large
657 Alignments. PLOS ONE. 2010 Mar 10;5(3):e9490.

658 23. Rambaut A, Lam TT, Max Carvalho L, Pybus OG. Exploring the temporal structure of
659 heterochronous sequences using TempEst (formerly Path-O-Gen). Virus Evol [Internet]. 2016 Jan
660 1 [cited 2017 Jun 14];2(1). Available from:
661 https://academic.oup.com/ve/article/2/1/vew007/1753488/Exploring-the-temporal-structure-
662 of-heterochronous

663 24. Bouckaert R, Vaughan TG, Barido-Sottani J, Duchêne S, Fourment M, Gavryushkina A, et al.
664 BEAST 2.5: An advanced software platform for Bayesian evolutionary analysis. PLOS Comput Biol.
665 2019 Apr 8;15(4):e1006650.

666 25. Wiser MJ, Lenski RE. A Comparison of methods to measure fitness in *Escherichia coli*. PLOS ONE.
667 2015 May 11;10(5):e0126210.

668 26. Abramson J, Adler J, Dunger J, Evans R, Green T, Pritzel A, et al. Accurate structure prediction of
669 biomolecular interactions with AlphaFold 3. Nature. 2024 Jun;630(8016):493–500.

670 27. Palace SG, Wang Y, Rubin DHF, Welsh MA, Mortimer TD, Cole K, et al. RNA polymerase
671 mutations cause cephalosporin resistance in clinical *Neisseria gonorrhoeae* isolates. Stallings CL,
672 Storz G, Shafer W, editors. eLife. 2020 Feb 3;9:e51407.

673 28. Panchal VV, Griffiths C, Mosaei H, Bilyk B, Sutton JAF, Carnell OT, et al. Evolving MRSA: High-level
674 β-lactam resistance in *Staphylococcus aureus* is associated with RNA Polymerase alterations and
675 fine tuning of gene expression. PLOS Pathog. 2020;16(7):e1008672.

676 29. Patel Y, Soni V, Rhee KY, Helmann JD. Mutations in *rpoB* that confer rifampicin resistance can
677 alter levels of peptidoglycan precursors and affect β-lactam susceptibility. mBio.
678 2023;14(2):e03168-22.

679 30. Fan Z, Chen H, Li M, Pan X, Fu W, Ren H, et al. *Pseudomonas aeruginosa* polynucleotide
680 phosphorylase contributes to ciprofloxacin resistance by regulating PrtR. Front Microbiol.
681 2019;10:1762.

682 31. Fan Z, Pan X, Wang D, Chen R, Fu T, Yang B, et al. *Pseudomonas aeruginosa* polynucleotide
683 phosphorylase controls tolerance to aminoglycoside antibiotics by regulating the MexXY
684 multidrug efflux pump. Antimicrob Agents Chemother. 2021 Jan 20;65(2).

685 32. Abavisani M, Keikha M, Karbalaei M. First global report about the prevalence of multi-drug
686 resistant Haemophilus influenzae: a systematic review and meta-analysis. BMC Infect Dis. 2024
687 Jan 15;24(1):90.

688 33. Apjok G, Boross G, Nyerges Á, Fekete G, Lázár V, Papp B, et al. Limited Evolutionary Conservation
689 of the Phenotypic Effects of Antibiotic Resistance Mutations. Mol Biol Evol. 2019 May
690 6;36(8):1601.

691 34. Osaki Y, Sanbongi Y, Ishikawa M, Kataoka H, Suzuki T, Maeda K, et al. Genetic approach to study
692 the relationship between penicillin-binding protein 3 mutations and *Haemophilus influenzae*
693 beta-lactam resistance by using site-directed mutagenesis and gene recombinants. Antimicrob
694 Agents Chemother. 2005 Jul;49(7):2834–9.

695 35. García-Cobos S, Campos J, Lázaro E, Román F, Cercenado E, García-Rey C, et al. Ampicillin-
696 resistant non-β-lactamase-producing *Haemophilus influenzae* in Spain: Recent emergence of

697 clonal isolates with increased resistance to cefotaxime and cefixime. Antimicrob Agents
698 Chemother. 2007;51(7):2564–73.

699 36. Straker K, Wootton M, Simm AM, Bennett PM, MacGowan AP, Walsh TR. Cefuroxime resistance
700 in non-β-lactamase *Haemophilus influenzae* is linked to mutations in *ftsI*. J Antimicrob
701 Chemother. 2003;51(3):523–30.

702 37. Slotved HC, Johannesen TB, Stegger M, Dalby T, Fuursted K. National Danish surveillance of
703 invasive clinical *Haemophilus influenzae* isolates and their resistance profile. Front Microbiol.
704 2023 Nov;14.

705 38. Skaare D, Allum AG, Anthonisen IL, Jenkins A, Lia A, Strand L, et al. Mutant *ftsI* genes in the
706 emergence of penicillin-binding proteinmediated β-lactam resistance in *Haemophilus influenzae*
707 in Norway. Clin Microbiol Infect. 2010 Aug 1;16(8):1117–24.

708 39. Thegerström J, Matuschek E, Su YC, Riesbeck K, Resman F. A novel PBP3 substitution in
709 *Haemophilus influenzae* confers reduced aminopenicillin susceptibility. BMC Microbiol. 2018
710 May 31;18(1):48.

711 40. Lâm TT, Claus H, Elias J, Frosch M, Vogel U. Ampicillin resistance of invasive *Haemophilus*
712 *influenzae* isolates in Germany 2009–2012. Int J Med Microbiol. 2015 Oct 1;305(7):748–55.

713 41. Diricks M, Petersen S, Bartels L, Lâm TT, Claus H, Bajanca-Lavado MP, et al. Revisiting mutational
714 resistance to ampicillin and cefotaxime in Haemophilus influenzae. Genome Med. 2024 Dec
715 4;16(1):140.

716 42. Skaare D, Anthonisen IL, Kahlmeter G, Matuschek E, Natås OB, Steinbakk M, et al. Emergence of
717 clonally related multidrug resistant Haemophilus influenzae with penicillin-binding protein 3-
718 mediated resistance to extended-spectrum cephalosporins, Norway, 2006 to 2013. Euro Surveill
719 Bull Eur Sur Mal Transm Eur Commun Dis Bull. 2014 Dec 11;19(49):20986.

720 43. Jakubu V, Vrbova I, Bitar I, Cechova M, Malisova L, Zemlickova H. Evolution of mutations in the
721 *ftsI* gene leading to amino acid substitutions in PBP3 in *Haemophilus influenzae* strains under the
722 selective pressure of ampicillin and cefuroxime. Int J Med Microbiol. 2024 Sep 1;316:151626.

723 44. Vachon V, D J Lyew, Coulton JW. Transmembrane permeability channels across the outer
724 membrane of *Haemophilus influenzae* type b. J Bacteriol. 1985;162(3):918–24.

725 45. Vachon V, Laprade R, Coulton JW. Properties of the porin of *Haemophilus influenzae* type b in
726 planar lipid bilayer membranes. Biochim Biophys Acta BBA - Biomembr. 1986 Jan 1;861:74–82.

727 46. Sikkema DJ, Murphy TF. Molecular analysis of the P2 porin protein of nontypeable *Haemophilus*
728 *influenzae*. Infect Immun. 1992;60(12):5204–11.

729 47. Duim B, Dankert J, Jansen HM, van Alphen L. Genetic analysis of the diversity in outer membrane
730 protein P2 of non-encapsulated *Haemophilus influenzae*. Microb Pathog. 1993 Jun 1;14(6):451–
731 62.

732 48. Bell J, Grass S, Jeanteur D, Munson RS. Diversity of the P2 protein among nontypeable
733 *Haemophilus influenzae* isolates. Infect Immun. 1994;62(6):2639–43.

734 49. Annette G. Regelink, David Dahan, Lieke V. M. Möller, James W. Coulton, Paul Eijk, Peter Van
735 Ulsen, et al. Variation in the composition and pore function of major outer membrane pore

736 protein P2 of *Haemophilus influenzae* from cystic fibrosis patients. Antimicrob Agents
737 Chemother. 1999;43(2):226–32.

738 50. Duim B, van Alphen L, Eijk P, Jansen HM, Dankert J. Antigenic drift of non-encapsulated
739 *Haemophilus influenzae* major outer membrane protein P2 in patients with chronic bronchitis is
740 caused by point mutations. Mol Microbiol. 1994 Mar 1;11(6):1181–9.

741 51. Duim B, Vogel L, Puijk W, Jansen HM, Meloen RH, Dankert J, et al. Fine mapping of outer
742 membrane protein P2 antigenic sites which vary during persistent infection by *Haemophilus*
743 *influenzae*. Infect Immun. 1996;64(11):4673–9.

744 52. Zwama M, Yamaguchi A, Nishino K. Phylogenetic and functional characterisation of the
745 *Haemophilus influenzae* multidrug efflux pump AcrB. Commun Biol. 2019 Sep 13;2(1):340.

746 53. Cherkaoui A, Diene SM, Renzoni A, Emonet S, Renzi G, François P, et al. Imipenem
747 heteroresistance in nontypeable *Haemophilus influenzae* is linked to a combination of altered
748 PBP3, slow drug influx and direct efflux regulation. Clin Microbiol Infect. 2017;23(2):118.e9-
749 118.e19.

750 54. Honda H, Sato T, Shinagawa M, Fukushima Y, Nakajima C, Suzuki Y, et al. *In vitro* derivation of
751 fluoroquinolone-resistant mutants from multiple lineages of *Haemophilus influenzae* and
752 identification of mutations associated with fluoroquinolone resistance. Antimicrob Agents
753 Chemother. 2020;64(2):10.1128/aac.01500-19.

754 55. Lou H, Chen M, Black SS, Bushell SR, Ceccarelli M, Mach T, et al. Altered antibiotic transport in
755 OmpC mutants isolated from a series of clinical strains of multi-drug resistant *E. coli*. PLoS One.
756 2011;6(10):e25825.

757 56. Raj Singh P, Ceccarelli M, Lovelle M, Winterhalter M, Mahendran KR. Antibiotic permeation
758 across the OmpF channel: Modulation of the affinity site in the presence of magnesium. J Phys
759 Chem B. 2012 Apr 19;116(15):4433–8.

760 57. Acosta-Gutierrez S, Scorciapino MA, Bodrenko I, Ceccarelli M. Filtering with electric field: The
761 case of *E. coli* porins. J Phys Chem Lett. 2015 May 21;6(10):1807–12.

762 58. Boonsiri T, Watanabe S, Tan XE, Thitiananpakorn K, Narimatsu R, Sasaki K, et al. Identification
763 and characterization of mutations responsible for the β-lactam resistance in oxacillin-susceptible
764 mecA-positive *Staphylococcus aureus*. Sci Rep. 2020 Oct 9;10(1):16907.

765 59. Card KJ, Thomas MD, Graves JL, Barrick JE, Lenski RE. Genomic evolution of antibiotic resistance
766 is contingent on genetic background following a long-term experiment with *Escherichia coli*. Proc
767 Natl Acad Sci. 2021 Feb 2;118(5):e2016886118.

768 60. Sulaiman Jordy E, Lam H. Novel daptomycin tolerance and resistance mutations in methicillin-
769 resistant *Staphylococcus aureus* from adaptive laboratory evolution. mSphere.
770 2021;6(5):10.1128/msphere.00692-21.

771 61. Wu J, Long Q, Xie J. (p)ppGpp and drug resistance. J Cell Physiol. 2010 Aug;224(2):300–4.

772 62. Nguyen D, Joshi-Datar A, Lepine F, Bauerle E, Olakanmi O, Beer K, et al. Active starvation
773 responses mediate antibiotic tolerance in biofilms and nutrient-limited bacteria. Science. 2011
774 Nov 18;334(6058):982–6.

775 63. Geng X, Li W, Chen Z, Gao S, Hong W, Ge X, et al. The bifunctional enzyme SpoT is involved in the
776 clarithromycin tolerance of *Helicobacter pylori* by upregulating the transporters HP0939,
777 HP1017, HP0497, and HP0471. Antimicrob Agents Chemother. 2017 May;61(5).

778 64. Andersson DI, Hughes D. Antibiotic resistance and its cost: is it possible to reverse resistance?
779 Nat Rev Microbiol. 2010 Apr 1;8(4):260–71.

780 65. Andersson DI, Levin BR. The biological cost of antibiotic resistance. Curr Opin Microbiol. 1999 Oct
781 1;2(5):489–93.

782 66. Melnyk AH, Wong A, Kassen R. The fitness costs of antibiotic resistance mutations. Evol Appl.
783 2015 Mar;8(3):273–83.

784 67. Hughes D, Andersson DI. Evolutionary trajectories to antibiotic resistance. Annu Rev Microbiol.
785 2017 Sep 8;71:579–96.

786 68. O'Neill AJ, Huovinen T, Fishwick CWG, Chopra I. Molecular genetic and structural modeling
787 studies of *Staphylococcus aureus* RNA polymerase and the fitness of rifampin resistance
788 genotypes in relation to clinical prevalence. Antimicrob Agents Chemother. 2006;50(1):298–309.

789 69. Böttger EC, Springer B, Pletschette M, Sander P. Fitness of antibiotic-resistant microorganisms
790 and compensatory mutations. Nat Med. 1998 Dec 1;4(12):1343–4.

791 70. Sander P, Springer B, Prammananan T, Sturmfels A, Kappler M, Pletschette M, et al. Fitness cost
792 of chromosomal drug resistance-conferring mutations. Antimicrob Agents Chemother.
793 2002;46(5):1204–11.

794 71. Gamblin J, Gandon S, Blanquart F, Lambert A. Bottlenecks can constrain and channel
795 evolutionary paths. Genetics. 2023;224(2):iyad001.

796 72. Wahl LM, Gerrish PJ. The probability that beneficial mutations are lost in populations with
797 periodic bottlenecks. Evolution. 2001;55(12):2606–10.

798 73. Mahrt N, Tietze A, Künzel S, Franzenburg S, Barbosa C, Jansen G, et al. Bottleneck size and
799 selection level reproducibly impact evolution of antibiotic resistance. Nat Ecol Evol. 2021
800 Sep;5(9):1233–42.

801 74. Andersen C, Maier E, Kemmer G, Blass J, Hilpert AK, Benz R, et al. Porin OmpP2 of *Haemophilus*
802 *influenzae* shows specificity for nicotinamide-derived nucleotide substrates. J Biol Chem. 2003 Jul
803 4;278(27):24269–76.

804 75. Evans NM, Smith DD, Wicken AJ. Haemin and nicotinamide adenine dinucleotide requirements
805 of *Haemophilus influenzae* and *Haemophilus parainfluenzae*. J Med Microbiol. 1974;7(3):359–65.

806 76. Fleischmann RD, Adams MD, White O, Clayton RA, Kirkness EF, Kerlavage AR, et al. Whole-
807 genome random sequencing and assembly of *Haemophilus influenzae* Rd. Science. 1995 Jul
808 28;269(5223):496–512.

809 77. Pennings PS, Ogbunugafor CB, Hershberg R. Reversion is most likely under high mutation supply
810 when compensatory mutations do not fully restore fitness costs. G3 GenesGenomesGenetics.
811 2022;12(9):jkac190.

812 78. Roemhild R, Andersson DI. Mechanisms and therapeutic potential of collateral sensitivity to
813 antibiotics. PLOS Pathog. 2021 Jan 14;17(1):e1009172.

814 79. Cazzola M, Blasi E, Allegra L. Critical evaluation of guidelines for the treatment of lower
815 respiratory tract bacterial infections. Respir Med. 2001 Feb;95(2):95–108.

816 80. Son JE, Park SH, Choi U, Lee CR. Lytic transglycosylase repertoire diversity enables intrinsic
817 antibiotic resistance and daughter cell separation in Escherichia coli under acidic stress.
818 Antimicrob Agents Chemother. 2024 Jun 17;68(7):e00372-24.

819 81. Le TA, Hiba T, Chaudhari D, Preston AN, Palowsky ZR, Ahmadzadeh S, et al. Aminoglycoside-
820 Related Nephrotoxicity and Ototoxicity in Clinical Practice: A Review of Pathophysiological
821 Mechanism and Treatment Options. Adv Ther. 2023 Apr 1;40(4):1357–65.

822

823

Supplementary Figures

Supplementary Figure S1: Graphical protocol of the performed multi-step evolution experiment (generated with BioRender).

Supplementary Figure S2: Graphical protocol of the performed competitive growth assay (generated with BioRender).

Supplementary Figure S3: Maximum likelihood phylogeny of *H. influenzae* Rd KW20 clones evolved in the absence of an antibiotic pressure (A, 40 clones) and in three replicate populations evolved in ceftriaxone (B, replicate 1 with 57 clones; C replicate 2 with 56 clones; D, replicate 3 with 59 clones). Amino acid substitutions in the penicillin binding protein 3 (PBP3) and presence of mutations in specified genes as well as minimum inhibitory concentration (MIC) changes over time are color coded. Strains that exceeded the clinical breakpoint for ampicillin/cefotaxime/ceftriaxone according to EUCAST breakpoints are marked with a white star at the MIC heatmap.
The specified genes are those in which at least 20 clones from the whole set of selected clones exhibited mutations but did not mutate under antibiotic-free conditions.

Supplementary Figure S4: Crystal structure of Outer membrane protein P2 of wild-type *H. influenzae* Rd KW20 (A) and mutated OmpP2 (B) truncated due to p.Thr126fs (c.376_377insT). Structures were predicted using the AlphaFold Server powerd by AlphaFold 3 (26) and visualized using PyMOL v3.0. Deviations between the two variants are highlighted in red.

Supplementary Figure S5: Crystal structure of Outer membrane protein P2 of wild-type *H. influenzae* Rd KW20, shown in side view (A) and bottom view (B) and two variants of OmpP2 altered due to p.Gly354fs (C and D, inversion) and p.Val353fs (E and F, deletion). Structures were predicted using the AlphaFold Server powerd by AlphaFold 3 (26) and visualized using PyMOL v3.0. Deviations between the two variants are labeled and highlighted in yellow (hydrophobic), green (polar uncharged), and blue (positively charged).

Supplementary Figure S6: Gradient diffusion test demonstrating phenotypic heterogeneity. The image shows two distinct inhibition zones surrounding the antibiotic gradient strip, indicative of a heterogeneous bacterial population. The inner zone corresponds to a subpopulation with higher antibiotic resistance, while the outer zone represents the more susceptible majority.